Contribution from the Department of Chemistry,
The University of Texas at Austin, Austin, Texas 78712

Electrochemistry and Photoelectrochemistry of Pillared-Clay-Modified Electrodes

Daiting Rong, Yeong Il Kim, and Thomas E. Mallouk*

Received September 14, 1989

Clay-modified electrodes (CME) were made by binding $Al_{13}O_4(OH)_{28}^{3+}$-pillared montmorillonite to SnO_2 and Pt surfaces via a thin (2–4 monolayer thick) coating of polymerized silane I. The polymer provides a binding site for multiply charged anions

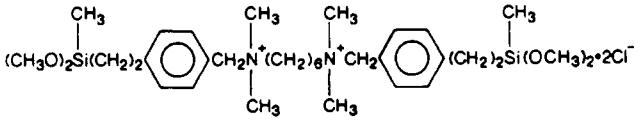

I

such as $Fe(CN)_6^{4-}$ and $Mo(CN)_8^{4-}$, while the clay external surface strongly binds large cations such as $Os(bpy)_3^{2+}$ and $Ru(bpy)_3^{2+}$. Charge-trapping behavior, which is a consequence of spatial ordering of the electroactive anions and cations, is observed in cyclic voltammetry of the CME in aqueous KH_2PO_4 solution. With $Ru(bpy)_3^{2+}$ exchanged onto the clay surface, photocathodic currents are generated with a quantum efficiency (per photon absorbed) of ca. 1%. This photocurrent is attributed to electron donor quenching of the $Ru(bpy)_3^{2+}$ excited state by $Fe(CN)_6^{4-}$ or $Mo(CN)_8^{4-}$.

Introduction

Smectite clays are interesting inorganic materials because they are useful (and almost literally dirt cheap) organizing media for chemical reactions. Many kinds of bimolecular organic reactions are accelerated by clay dispersions simply because the reactants can encounter each other more frequently when they are confined to the two-dimensional surface of clay lamellae.[1] Complex, multicomponent chemical systems with unusual catalytic properties can be prepared on clay surfaces. For example, Van Damme and co-workers have shown that integrated systems for water photolysis, which contain photosensitizers, electron relays, and catalyst particles, can be prepared by using clays as the organizing matrix.[2]

By exchanging clays with pillaring ions of well-defined size[3] (e.g. $Al_{13}O_4(OH)_{28}^{3+}$ or $Zr_4(OH)_{16-x}^{x+}$), one can impart an additional molecular-sieving property: ions and molecules larger than the pillar height cannot enter the interlamellar region. This property is particularly useful for size- or shape-selective catalysis.[4] It can also be exploited, in combination with the ability of clays to exchange cations, in the preparation of supramolecular systems, which spontaneously organize themselves according to the size and charge of their molecular components. Using similar microporous organizing media (zeolites), we and others have shown that two- and three-component electroactive systems can be made to self-assemble simply by choosing ions of the appropriate size, charge, and shape.[5-7] Good spatial organization in these systems can be inferred from electrochemical effects such as current rectification[5a] and charge trapping[5b] and from observations of photochemically driven vectorial electron transport.[5d,e] In this paper we show that electrochemical and photoelectrochemical effects indicative of molecular self-organization can also be obtained at pillared-clay-modified electrodes.

Previous studies of clay-modified electrodes (CME) and electrodes prepared with structurally related hydrotalcite (layered double hydroxides) have emphasized the role of the layered solid as an inorganic ion exchanger[8] and as a host for chiral[9] and electrocatalytic[10] reactions. The preparation of structurally well-organized molecular assemblies at a CME has not yet been explored. We report here that electrochemical charge trapping and light-driven vectorial electron transport occur at CME's prepared according to Scheme I. By use of a cationic silane molecule (I), a thin layer of pillared-clay particles can be tethered

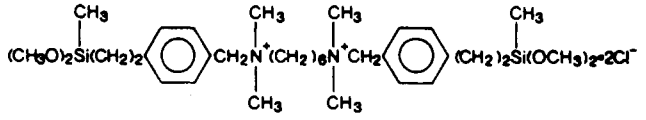

I

to the surface of an electrode. The fixed positive charges of the silane provide a binding site for multiply charged anions, while

Scheme I. CME Preparation and Ion Exchange of a Bimolecular Redox Assembly

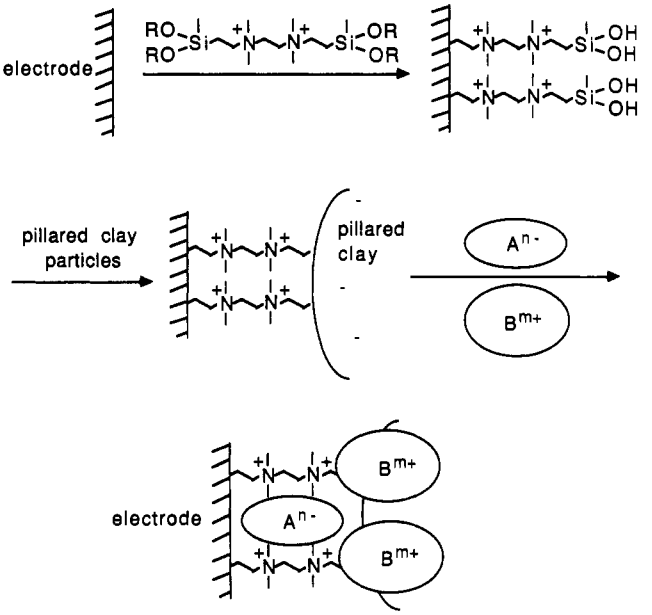

* To whom correspondence should be addressed.

(1) (a) Laszlo, P. *Acc. Chem. Res.* **1986**, *19*, 121. (b) Laszlo, P. *Science* **1987**, *235*, 1473. (c) Thomas, J. M. In *Intercalation Chemistry*; Jacobson, A. J., Whittingham, M. S., Eds.; Academic Press: New York, 1982; pp 55–89.
(2) (a) Nijs, H.; Fripiat, J. J.; Van Damme, H. *J. Phys. Chem.* **1983**, *87*, 1279. (b) Nijs, H.; Cruz, M.; Fripiat, J.; Van Damme, H. *J. Chem. Soc., Chem. Commun.* **1981**, 1026. (c) Krenske, D.; Abdo, S.; Van Damme, H.; Cruz, M.; Fripiat, J. J. *J. Phys. Chem.* **1980**, *84*, 2447.
(3) (a) Barrer, R. M.; MacLeod, D. M. *Trans. Faraday Soc.* **1955**, *51*, 1290. (b) Kellendonk, F. J. A.; Heinerman, J. J. L.; van Santen, R. A. In *An Introduction to Clay Colloid Chemistry*; van Olphen, H., Ed.; Wiley: New York, 1977; p 459 and references therein. (c) Brindley, G. W.; Sempels, R. E. *Clay Miner.* **1977**, *12*, 229. (d) Yamanaka, S.; Brindley, G. W. *Clays Clay Miner.* **1978**, *26*, 21.
(4) Pinnavaia, T. J. *Science* **1983**, *220*, 365.
(5) (a) Li, Z.; Mallouk, T. E. *J. Phys. Chem.* **1987**, *91*, 643. (b) Li, A.; Wang, C. M.; Persaud, L.; Mallouk, T. E. *J. Phys. Chem.* **1988**, *92*, 2592. (c) Li, Z.; Lai, C.; Mallouk, T. E. *Inorg. Chem.* **1989**, *28*, 178. (d) Persaud, L.; Bard, A. J.; Campion, A.; Fox, M. A.; Mallouk, T. E.; Webber, S. E.; White, J. M. *J. Am. Chem. Soc.* **1987**, *109*, 7309. (e) Krueger, J. S.; Mayer, J. E.; Mallouk, T. E. *J. Am. Chem. Soc.* **1988**, *110*, 8232. (f) Krueger, J. S.; Lai, C.; Li, Z.; Mayer, J. E.; Mallouk, T. E. *Proceedings of the 5th International Symposium on Inclusion Phenomena and Molecular Recognition*; Atwood, J. L., Ed.; in press.
(6) Faulkner, L. R.; Suib, S. L.; Renschler, C. L.; Green, J. M.; Bross, P. R. In *Chemistry in Energy Production*; Wymer, R. G., Keller, O. L., Eds.; Wiley: New York, 1982; pp 99–114.

0020-1669/90/1329-1531$02.50/0

electroactive cations larger than the pillar height (ca. 9 Å) adhere to the external surface of the clay. The CME differs from similarly prepared zeolite-modified electrodes[5c] in that large electroactive cations are more strongly bound by the clay surface. This property is advantageous because it gives rise to better spatial ordering of the electroactive anions and cations, as manifested in both electrochemical and photoelectrochemical experiments.

Experimental Section

Materials. Texas montmorillonite (STx-1) was obtained from the Source Clay Minerals Repository (University of Missouri, Columbia, MO). It was ion-exchanged and pillared by using a modification of the procedure described by Rudzinski and Bard.[8g] The clay was converted from the Ca^{2+} to Na^+ form by stirring with 1 M aqueous NaCl for 3–4 days. This was followed by sequential washing with deionized water (from a Barnstead Nanopure II system, resistivity 18.3 MΩ cm) and centrifugation to remove excess NaCl. A chlorhydrol solution, $[Al(OH)_2Cl]_x$, was prepared by slowly adding 0.05 M NaOH with vigorous stirring to 0.1 M $AlCl_3$, until a 2/1 stoichiometry of Na/Al was reached. A 5-mL aliquot of the resulting 0.02 N $[Al(OH)_2Cl]_x$ was added to 5 mL of an aqueous Na^+–STx-1 suspension (10 g/L). The mixture was allowed to react overnight, and the sample was then centrifuged and air-dried at 120 °C. $K_4Mo(CN)_8 \cdot 2H_2O$ was prepared as described by Furman and Miller.[11] Tris(2,2′-bipyridine)osmium(II) perchlorate was synthesized by the method of Gaudiello et al.,[12] and tris(2,2′-bipyridine)ruthenium(II) chloride hexahydrate was obtained from Aldrich Chemical Co. and used as received. Acetonitrile (HPLC grade) was freshly distilled from P_2O_5 before use. Compound I was available from previous experiments.[5c] All other chemicals were of reagent grade quality and were obtained from commercial sources.

Electrode Preparation and Ion Exchange. Conductive SnO_2-on-glass electrodes were prepared and cleaned as previously described.[5a-c] Platinum foil electrodes were prepared similarly but were cleaned electrochemically in 0.5 M H_2SO_4 by holding for several minutes at +2.0 V vs SCE, followed by cycling at 100 mV/s between the hydrogen (−0.25 V) and oxygen (+1.1 V) evolution potentials; the final potential was +1.1 V, and the electrodes were then rinsed with deionized water and air-dried. Electrodes were immersed in a 1 mM solution of I in acetonitrile for 1–3 days and were then transferred to a stirred solution of the pillared clay (0.01 g in 10 mL of acetonitrile) for 2 days. These steps were carried out at room temperature. The electrodes were removed from the suspension, dipped in acetonitrile, and dried at 120 °C in air. Ion exchange was carried out by immersing the electrode for several hours in 1 mM aqueous solutions of compounds containing the appropriate ions, i.e. $K_4Fe(CN)_6 \cdot 3H_2O$, $K_4Mo(CN)_8 \cdot 2H_2O$, $Os(bpy)_3(ClO4)_2$, and $Ru(bpy)_3Cl_2 \cdot 6H_2O$.

Apparatus. Electrochemical experiments were carried out in 1 mM aqueous KH_2PO_4 by using a one-compartment, three-electrode cell, as described previously.[5a-c] All potentials are referenced to the saturated calomel electrode (SCE) and are uncorrected for *iR* drop and liquid junction potentials. UV–visible spectra of transparent SnO_2/glass electrodes were obtained with an HP8451A diode array spectrophotometer. Diffuse-reflectance UV–vis spectra were taken with a DMS-300 instrument equipped with an integrating sphere attachment. Emission spectra were collected with a Spex Fluorolog spectrometer interfaced to a Tracor Northern TN-6500 diode array detector. For photochemical experiments a 100-W xenon arc lamp was used, with either a 400-nm low-pass filter or a Jarrell-Ash Model 82560 monochromator. Light intensities were measured with an EG&G Model 550-1 radiometer. X-ray powder diffraction patterns were obtained as previously described.[13]

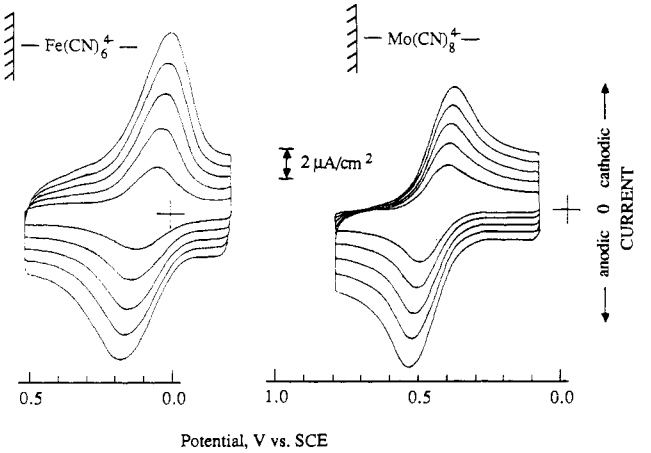

Figure 1. Cyclic voltammetry in 1 mM aqueous KH_2PO_4 of SnO_2/I/pillared-clay electrodes ion-exchanged with ferrocyanide (left) and octacyanomolybdate (right). Scan rates are 20, 40, 60, 80, and 100 mV/s. Integration at slow scan rate gives $\Gamma_{Fe(CN)_6^{4-}} = 1.3 \times 10^{-10}$ and $\Gamma_{Mo(CN)_8^{4-}} = 9.1 \times 10^{-11}$ mol/cm².

Results and Discussion

Electrode Structure. Pillaring of clay particles with $[Al(OH)_2Cl]_x$ solution causes flocculation of the originally well-dispersed montmorillonite. Electron micrographs show that the pillared particles are lamellar, with approximate dimensions of 1–2 μm × 0.05–0.1 μm. X-ray diffraction patterns of the pillared clay showed a (001) reflection corresponding to a repeat distance of 19 Å along the stacking axis, which is consistent with previous reports[3,4,8g] of 17–19 Å for $Al_{13}O_4(OH)_{28}^{3+}$-pillared montmorillonite. Since the basal plane spacing of fully dehydrated calcium montmorillonite is approximately 10 Å, a free gallery height of ca. 9 Å is implied for our material. Electron micrographs of the derivitized electrode show that these particles are bound as a patchy thin film that covers about two-thirds of the surface. Individual grains appear to have a random orientation relative to the surface plane.

Electrochemistry. Functionalization of electrode surfaces with I gives a siloxane polymer layer that is on the order of 2–4 monolayers thick.[5c] This polymer presumably contains some free silanol groups, which are capable of binding aluminosilicate (zeolite or clay) particles through siloxane (Si–O–Si) linkages. This arrangement gives anion-exchange sites, associated with the fixed positive charges of I, very near the electrode surface and more remote cation binding sites associated with the aluminosilicate particles. Accordingly, when these films are exchanged with multiply charged electroactive cations and cycled in a blank electrolyte solution, the reversible oxidation and reduction of these ions can be observed. Figure 1 shows typical cyclic voltammetric traces obtained with $Fe(CN)_6^{4-}$- and $Mo(CN)_8^{4-}$-exchanged electrodes. Quasireversible oxidation/reduction waves are seen for both surface-confined redox couples. At low scan rates the anodic peak current density is linear with scan rate, which is characteristic of a surface-confined couple, and integration gives a coverage of about 1×10^{-10} mol of electroactive ion/cm².

When these electrodes are exchanged with both $Fe(CN)_6^{4-}$ and large electroactive cations (e.g. $Os(bpy)_3^{2+}$), interesting effects are observed, as shown in Figure 2. $Os(bpy)_3^{2+}$ is clearly bound

(7) de Vismes, B.; Bedioui, F.; Devynck, J.; Bied-Charreton, C.; Perrée-Fauvet, M. *Nouv. J. Chim.* **1986**, *10*, 81.
(8) (a) Ghosh, P. K.; Bard, A. J. *J. Am. Chem. Soc.* **1983**, *105*, 5691. (b) Kamat, P. V. *J. Electroanal. Chem. Interfacial Electrochem.* **1984**, *163*, 389. (c) Ege, D.; Ghosh, P. K.; White, J. R.; Equey, J. F.; Bard, A. J. *J. Am. Chem. Soc.* **1985**, *107*, 5644. (d) Liu, H. Y.; Anson, F. C. *J. Electroanal. Chem. Interfacial Electrochem.* **1985**, *184*, 411. (e) White, J. R.; Bard, A. J. *J. Electroanal. Chem. Interfacial Electrochem.* **1986**, *197*, 233. (f) Itaya, K.; Bard, A. J. *J. Phys. Chem.* **1985**, *89*, 5565. (g) Rudzinski, W. E.; Bard, A. J. *J. Electroanal. Chem. Interfacial Electrochem.* **1986**, *199*, 323. (h) Carter, M. T.; Bard, A. J. *J. Electroanal. Chem. Interfacial Electrochem.* **1987**, *229*, 191. (i) Castro-Acuña, C. M.; Fan, F.-R. F.; Bard, A. J. *J. Electroanal. Chem. Interfacial Electrochem.* **1987**, *234*, 347. (j) King, R. D.; Nocera, D. G.; Pinnavaia, T. J. *J. Electroanal. Chem. Interfacial Electrochem.* **1987**, *236*, 43. (k) Itaya, K.; Chang, H. C.; Uchida, I. *Inorg. Chem.* **1987**, *26*, 624.
(9) (a) Yamagishi, A.; Aramata, A. *J. Chem. Soc., Chem. Commun.* **1984**, 452. (b) Yamagishi, A.; Aramata, A. *J. Electroanal. Chem. Interfacial Electrochem.* **1985**, *191*, 449. (c) Fitch, A.; Lavy-Feder, A.; Lee, S. A.; Kirsh, M. T. *J. Phys. Chem.* **1988**, *92*, 6665.
(10) (a) Ghosh, P. K.; Mau, A. W.-H.; Bard, A. J. *J. Electroanal. Chem. Interfacial Electrochem.* **1984**, *169*, 315. (b) Oyama, N.; Anson, F. C. *J. Electroanal. Chem. Interfacial Electrochem.* **1986**, *199*, 467. (c) Shaw, B. R.; Creasy, K. E. *J. Electroanal. Chem. Interfacial Electrochem.* **1988**, *243*, 209.
(11) Furman, N. H.; Miller, C. O. *Inorg. Synth.* **1950**, *3*, 160.
(12) Gaudiello, J. G.; Bradley, P. G.; Norton, K. A.; Woodruff, W. H.; Bard, A. J. *Inorg. Chem.* **1984**, *23*, 3.
(13) Cao, G.; Lee, H.; Lynch, V. M.; Mallouk, T. E. *Inorg. Chem.* **1988**, *27*, 2781.

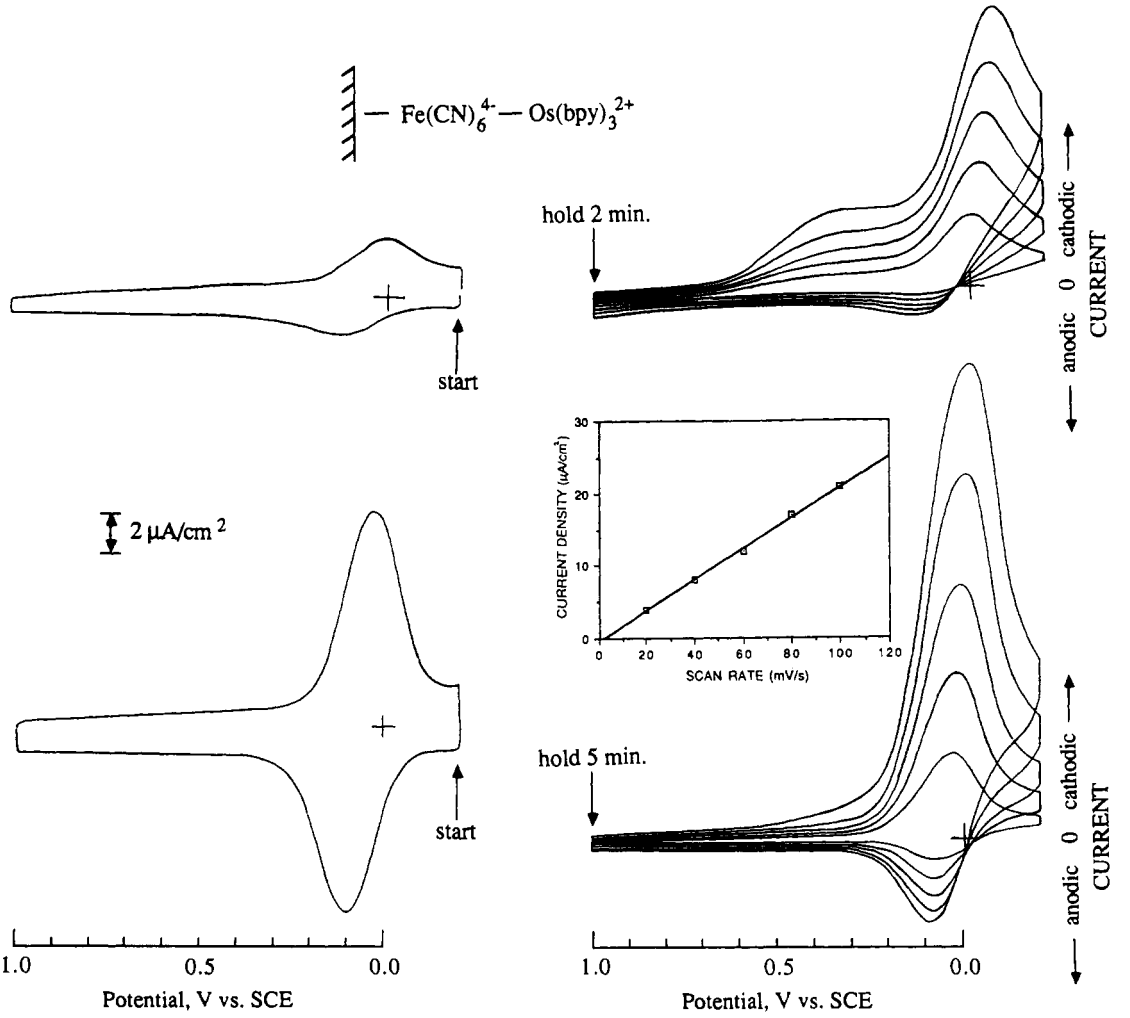

Figure 2. Cyclic voltammetry of a CME exchanged with both $Fe(CN)_6^{4-}$ and $Os(bpy)_3^{2+}$: (left side) scans initiated after prolonged hold at −0.2 V; (right side) scans initiated after hold at +1.0 V; (upper traces) $\Gamma_{Fe(CN)_6^{4-}} = 1.0 \times 10^{-10}$ mol/cm²; (lower traces) $\Gamma_{Fe(CN)_6^{4-}} = 1.6 \times 10^{-10}$ mol/cm²; (inset) plot showing the linear relation of peak current density and scan rate for the cathodic wave at lower right. Scan rates are 40 mV/s (upper left), 100 mV/s (lower left), and 20, 40, 60, 80, and 100 mV/s (right).

by the polymer/clay film, as the electrode surface acquires the green color of the complex. However, in cyclic voltammetric scans initiated at negative potentials (left traces in Figure 2), one sees waves attributable only to the $Fe(CN)_6^{4-/3-}$ interconversion; there is no apparent contribution from the $Os(bpy)_3^{2+/3+}$ couple, even though the electrode is swept well past its formal potential (+0.60 V). Holding the electrode for prolonged periods at very positive potential (+1.0 V) causes a pronounced change in the cyclic voltammogram (right traces in Figure 2). In this case the cathodic current is significantly enhanced. When the polymer film is very thin ($\Gamma_{Fe(CN)_6^{4-}} \leq 10^{-10}$ mol/cm²), the onset of the extra cathodic current lies near the $Os(bpy)_3^{2+/3+}$ potential. With slightly thicker polymer coatings the extra cathodic current is simply added to the $Fe(CN)_6^{3-} \rightarrow Fe(CN)_6^{4-}$ wave.

This behavior arises because of a "charge-trapping" phenomenon, which is a consequence of spatial ordering of $Fe(CN)_6^{4-}$ and $Os(bpy)_3^{2+}$. Similar effects are well documented for electrodes modified with bilayer polymer films,[14] films containing both fast and slow redox couples,[15,16] and modified electrodes in which one electroactive group is attached only to the outer surface of a polymer film.[17] Since the $Fe(CN)_6^{4-/3-}$ couple is held by the polymer layer near the electrode surface, reaction 1 and its reverse

$$Fe(CN)_6^{3-} + e^- = Fe(CN)_6^{4-} \quad (1)$$

are both facile. On the other hand, direction oxidation and reduction of $Os(bpy)_3^{3+/2+}$, reaction 2, is expected to be very slow

$$Os(bpy)_3^{3+} + e^- = Os(bpy)_3^{2+} \quad (2)$$

because the cation binding sites are too distant for rapid electron tunneling between $Os(bpy)_3^{3+/2+}$ and the electrode surface. The interconversion of the $Os(bpy)_3^{3+/2+}$ forms is mediated by the $Fe(CN)_6^{4-/3-}$ ions via reaction 3. In the forward direction this

$$Fe(CN)_6^{4-} + Os(bpy)_3^{3+} = Fe(CN)_6^{3-} + Os(bpy)_3^{2+} \quad (3)$$

reaction is very fast because it is thermodynamically favored by ca. 400 mV. Therefore, mediated reduction of $Os(bpy)_3^{3+}$ can occur easily, by a combination of (3) and (1). However, mediated oxidation of $Os(bpy)_3^{2+}$ is not observable on the time scale of cyclic voltammetry since the reversal of (3) is ca. 10^7 times slower than the forward reaction.

(14) (a) Abruña, H. D.; Denisevich, P.; Umana, M.; Meyer, T. J.; Murray, R. W. *J. Am. Chem. Soc.* **1981**, *103*, 1. (b) Denisevich, R.; Willman, K. W.; Murray, R. W. *J. Am. Chem. Soc.* **1981**, *103*, 4727. (c) Willman, K. W.; Murray, R. W. *J. Electroanal. Chem. Interfacial Electrochem.* **1982**, *133*, 211. (d) Pickup, P. G.; Leidner, C. R.; Denisevich, P.; Murray, R. W. *J. Electrochem. Soc.* **1984**, *164*, 39. (e) Pickup, P. G.; Kutner, W.; Leidner, C. R.; Murray, R. W. *J. Am. Chem. Soc.* **1984**, *106*, 1991. (f) Leidner, C. R.; Murray, R. W. *J. Am. Chem. Soc.* **1985**, *107*, 551.

(15) Fukui, M.; Kitami, A.; Degrand, C.; Miller, L. L. *J. Am. Chem. Soc.* **1982**, *104*, 28.

(16) (a) Buttry, D. A.; Anson, F. C. *J. Am. Chem. Soc.* **1984**, *106*, 59. (b) Anson, F. C.; Ni, C.-L.; Savéant, J.-M. *J. Am. Chem. Soc.* **1985**, *107*, 3442.

(17) (a) Hupp, J. T.; Otruba, J. P.; Parus, S. J.; Meyer, T. J. *J. Electroanal. Chem. Interfacial Electrochem.* **1985**, *190*, 287. (b) Surridge, N.; Hupp, J. T.; McClanahan, S.; Gould, S.; Meyer, T. J. *J. Phys. Chem.* **1989**, *93*, 294. (c) Surridge, N.; Hupp, J. T.; Danielson, E.; McClanahan, S.; Gould, S.; Meyer, T. J. *J. Phys. Chem.* **1989**, *93*, 304.

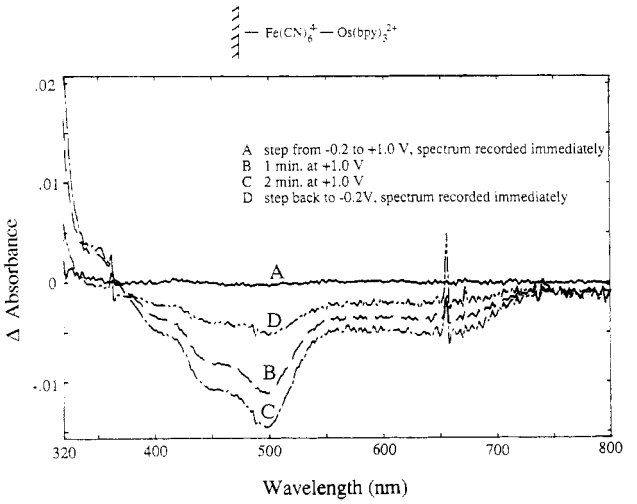

Figure 3. UV–visible difference spectra of the CME exchanged with both $Fe(CN)_6^{4-}$ and $Os(bpy)_3^{2+}$. Reference: same electrode held at −0.2 V vs SCE. Spectra A, B, and C were recorded 0, 1, and 2 min after stepping the electrode potential to +1.0 V. Spectrum D was recorded immediately after returning the potential to −0.2 V.

With very thin polymer films (upper right trace in Figure 2), there is direct reduction of $Os(bpy)_3^{3+}$ at the electrode surface, although there is no evidence for direct oxidation of $Os(bpy)_3^{2+}$. This suggests that $Os(bpy)_3^{2+}$ is bound more strongly by the clay than is $Os(bpy)_3^{3+}$ and that the latter can permeate the polymer film to some extent. The reason for weaker binding of $Os(bpy)_3^{3+}$, relative to $Os(bpy)_3^{2+}$, is unclear; we tentatively ascribe it to the low charge density and hydrophobic nature of the clay surface. With slightly thicker polymer films (lower traces, Figure 2), interconversion of $Os(bpy)_3^{3+/2+}$ is only possible via mediation, i.e., reaction 3. Consequently, oxidizing equivalents are "trapped" on the $Os(bpy)_3^{3+}$ sites until the electrode is returned to the $Fe(CN)_6^{4-/3-}$ potential. When the scan is initiated at negative potentials, no $Os(bpy)_3^{3+}$ can accumulate in the film during the brief anodic scan, since the reversal of (3) is so slow. However, holding the electrode for several minutes at +1.0 V causes enough $Os(bpy)_3^{3+}$ to accumulate (via the reverse of (3) or by direct tunneling from $Os(bpy)_3^{2+}$ to the electrode) that it can be observed in the cathodic sweep. The dependence of this cathodic peak current on scan rate is linear, as predicted theoretically for charge-trapping/charge-untrapping waves with thin polymer bilayer films.[14d]

The assignment of trapped redox equivalents to the $Os(bpy)_3^{2+/3+}$ couple can be confirmed by spectroelectrochemical experiments. Figure 3 shows difference spectra (the reference being a fully reduced electrode film) obtained by stepping abruptly past the $Os(bpy)_3^{2+/3+}$ and $Fe(CN)_6^{3-/4-}$ formal potentials. Stepping to positive potentials results in the slow loss of $Os(bpy)_3^{2+}$, as evidenced by negative ΔA features at 500 and 650 nm. The regeneration of $Os(bpy)_3^{2+}$, via (3), is very rapid, and about 60% of the $Os(bpy)_3^{3+}$ formed during a 2-min hold at +1.0 V is reduced within 1–2 s at −0.2 V.

With analogous electrode films prepared from I and zeolite Y, no charge trapping was found because of ion pairing between $Fe(CN)_6^{4-/3-}$ and $Os(bpy)_3^{2+/3+}$. In that case the ion pairs did not adhere strongly to the zeolite surface and were able to permeate the polymer film. Apparently, ion pairing is not competitive with surface binding of $Os(bpy)_3^{2+/3+}$ in the case of the pillared clay. Qualitative ion-exchange experiments carried out with $Ru(bpy)_3^{2+}$ show that at maximum loading (1.5×10^{-5} mol/g of pillared clay) it is not displaced by 2–3 M Na^+. Under these conditions $Ru(bpy)_3^{2+}$ is quantitatively removed from the external surface of zeolite Y.

Photoelectrochemical Effects. The good structural integrity of the $Fe(CN)_6^{4-}/Os(bpy)_3^{2+}$ bilayer obtained with I/pillared-clay electrodes suggests the possibility of photochemically driven vectorial electron transport. Replacing the $Os(bpy)_3^{2+}$ ions by $Ru(bpy)_3^{2+}$, one observes a modest cathodic photoeffect with either

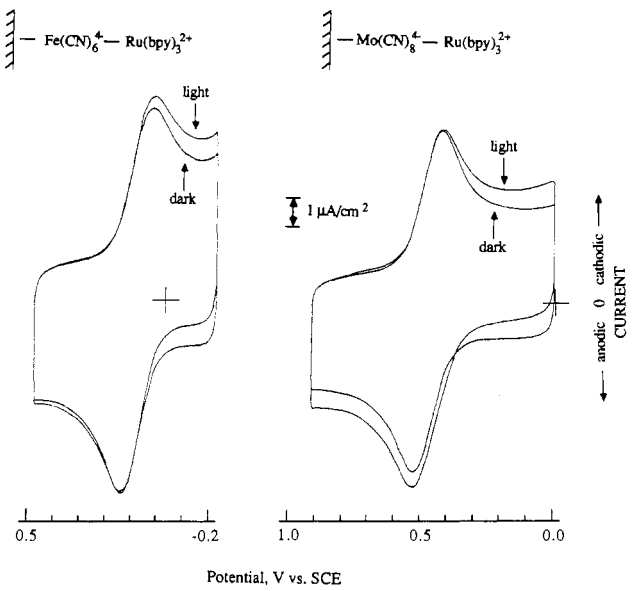

Figure 4. Cyclic voltammetry of SnO_2/anion/$Ru(bpy)_3^{2+}$ CME's with and without visible light illumination in 1 mM KH_2PO_4 (scan rate 100 mV/s): (left) $\Gamma_{Fe(CN)_6^{4-}} = 8.0 \times 10^{-11}$ mol/cm²; (right) $\Gamma_{Mo(CN)_8^{4-}} = 9.6 \times 10^{-11}$ mol/cm². Light source was a xenon arc lamp with 400-nm filter.

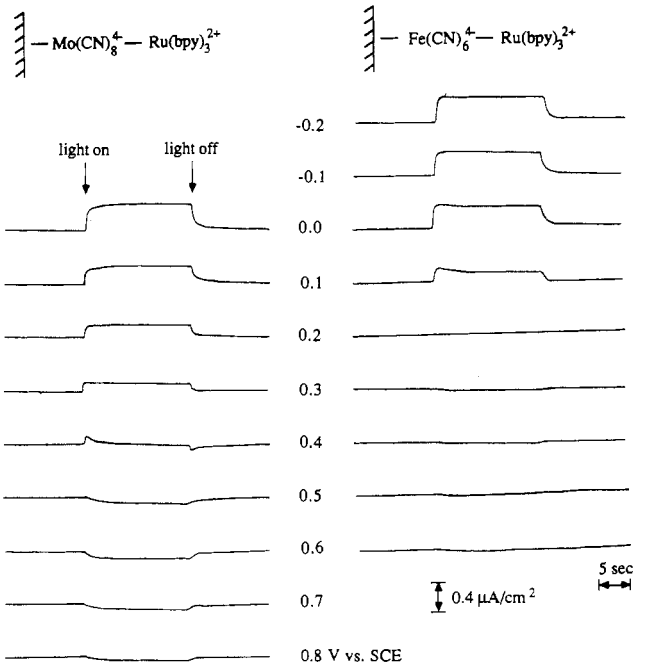

Figure 5. Photocurrent/time response for SnO_2/anion/$Ru(bpy)_3^{2+}$ CME's held at various potentials vs SCE: (left) $Mo(CN)_8^{4-}$; (right) $Fe(CN)_6^{4-}$.

$Fe(CN)_6^{4-}$ or $Mo(CN)_8^{4-}$ ions exchanged into the polymer. Figure 4 shows the cyclic voltammograms of these electrodes recorded with and without visible light illumination. This effect may be seen more clearly in Figure 5, in which the electrode is held at various potentials and the light is switched on and off. In both cases the onset of cathodic photocurrent lies near the formal potential of the anion ($Fe(CN)_6^{4-}$ or $Mo(CN)_8^{4-}$) bound by the layer of polymerized I at the electrode surface. No photocurrent is observed in the absence of either the anions or $Ru(bpy)_3^{2+}$. Similar photoeffects have been noted by Oyama and co-workers,[18] who studied the photochemistry of bilayer film electrodes prepared from polymeric derivatives of $Ru(bpy)_3^{2+}$ and methylviologen. The magnitude of the photocathodic effect shown in Figure 5 is suf-

(18) Oyama, N.; Yamaguchi, S.; Kaneko, M.; Yamada, A. *J. Electroanal. Chem. Interfacial Electrochem.* **1982**, *139*, 215.

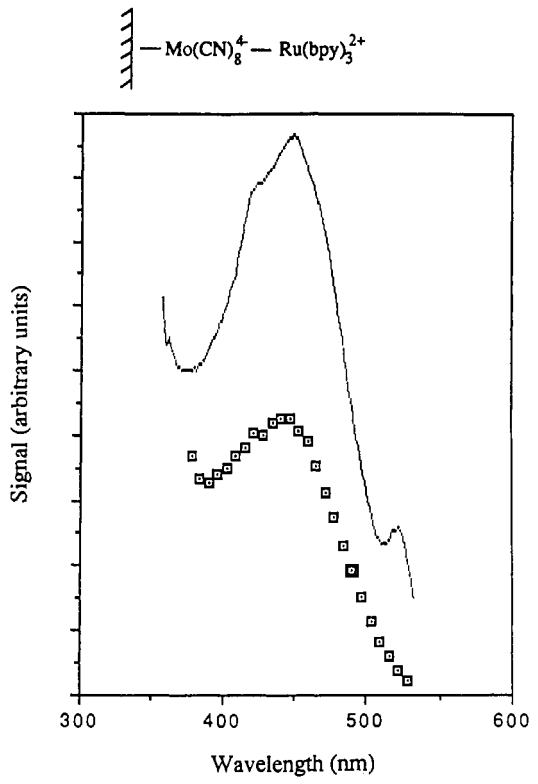

Figure 6. Normalized plot of photocurrent density vs wavelength for a $SnO_2/Mo(CN)_8^{4-}/Ru(bpy)_3^{2+}$ CME at 0.0 V vs SCE (lower, squares) and diffuse-reflectance spectrum of $Ru(bpy)_3^{2+}$/STx-1 (upper, dashed line).

ficiently small that only a few percent of the $Ru(bpy)_3^{2+}$ molecules adsorbed onto the surface of the clay are reduced in the time scale of the experiment; therefore an apparently constant photocurrent is observed during the short time that the light is on at each potential.

These observations are consistent with reductive electron-transfer quenching of excited-state $Ru(bpy)_3^{2+}$ by $Fe(CN)_6^{4-}$ or $Mo(CN)_8^{4-}$, i.e. reactions 4 and 5. The oxidized anion ($Fe(CN)_6^{3-}$

$$Fe(CN)_6^{4-} + {}^*Ru(bpy)_3^{2+} \rightarrow Fe(CN)_6^{3-} + Ru(bpy)_3^{+} \quad (4)$$

$$Mo(CN)_8^{4-} + {}^*Ru(bpy)_3^{2+} \rightarrow Mo(CN)_8^{3-} + Ru(bpy)_3^{+} \quad (5)$$

or $Mo(CN)_8^{3-}$) produced in this way is reduced if the electrode is held negative of its formal potential, via (1) or (6). Inter-

$$Mo(CN)_8^{3-} + e^- = Mo(CN)_8^{4-} \quad (6)$$

estingly, when the electrode containing $Mo(CN)_8^{4-/3-}$ is held positive of the formal potential of that couple, small photoanodic currents are observed. This current may arise from oxidative quenching of $*Ru(bpy)_3^{2+}$, via (7), coupled with an electrode reaction, which is the reverse of (6).

$$Mo(CN)_8^{3-} + {}^*Ru(bpy)_3^{2+} \rightarrow Mo(CN)_8^{4-} + Ru(bpy)_3^{3+} \quad (7)$$

In order to assess the efficiency of the photocathodic process and to confirm that excitation of $Ru(bpy)_3^{2+}$ is responsible for the observed current, experiments were carried out with monochromic light. In Figure 6 the photocurrent action spectrum of a $Mo(CN)_8^{4-}/Ru(bpy)_3^{2+}$-exchanged CME is compared with the diffuse-reflectance spectrum of $Ru(bpy)_3^{2+}$-exchanged STx-1. The close correspondence of these spectra indicates that light absorption by $Ru(bpy)_3^{2+}$, and not by $Fe(CN)_6^{4-}$ or $Mo(CN)_8^{4-}$, gives rise to the photocurrent.

From the absorption spectrum of the CME a photocurrent quantum efficiency (electrons per photon absorbed) of ca. 1% is calculated at 450 nm from the data represented in Figure 6. Emission quenching of the $Ru(bpy)_3^{2+}$-exchanged CME by $Fe(CN)_6^{4-}$ and $Mo(CN)_8^{4-}$ exchanged into the polymerized layer of I occurs with a quantum efficiency of approximately 15–30%[19] at 0.0 V vs SCE; therefore the low photocurrent efficiency can be attributed only partly to inefficient quenching. It is known from previous work[20] that, in homogeneous aqueous solution, the quantum efficiency for formation and cage escape of oxidized anion/$Ru(bpy)_3^{+}$ pairs is ca. 3% for $Fe(CN)_6^{3-}$ and 87% for $Mo(CN)_8^{3-}$. Surprisingly, photocurrent efficiencies are very similar for the two anions in the case of the CME.

In fluid aqueous solution, the large difference in cage escape efficiency between $Mo(CN)_8^{3-}$ and $Fe(CN)_6^{3-}$ is thought to arise because of the relative sizes of the two anions. Structuring of water molecules around $Mo(CN)_8^{4-/3-}$, through hydrogen bonding, may make for a "loose" ion pair with $Ru(bpy)_3^{2+/+}$, permitting efficient cage escape. Sheathing of the smaller $Fe(CN)_6^{4-/3-}$ ions by water may be less efficient, causing tighter pairing with $Ru(bpy)_3^{2+/+}$ and more rapid back electron transfer within the geminate ion pair. This hypothesis is supported by the observation[21] of a large positive volume of activation for quenching of $*Ru(bpy)_3^{2+}$ by $Mo(CN)_8^{4-}$ and essentially zero activation volume for quenching by $Fe(CN)_6^{4-}$. In the case of the CME, the anions are bound by the layer of polymerized I, which may not allow for complete aquation of the $Mo(CN)_8^{4-/3-}$ ions; therefore, for both $Mo(CN)_8^{4-/3-}$ and $Fe(CN)_6^{4-/3-}$ the quantum yield for charge separation is low, resembling that found for $Fe(CN)_6^{4-/3-}$ in aqueous solution.

Conclusions

We have demonstrated that a bimolecular electron-transport chain assembles spontaneously at electrodes functionalized with I and pillared-clay particles. Electron transfer along this chain can be driven either electrochemically, in which case a charge-trapping effect is observed, or photoelectrochemically. While we have explored here only bimolecular self-assembling systems, the pillared clay also contains zeolitic internal binding sites for small ions or molecules, and it may be possible therefore to add a third component to the chain.[5c] The low quantum efficiency for photocathodic current obtained with the CME (1% on a per-photon-absorbed basis) is attributed to tight geminate ion pairing of electron donor and acceptor ions, which may be a consequence of poor hydration of the anions within the polymerized layer of I. More hydrophilic polymers, e.g. the cationic polyelectrolytes recently reported by Anson and co-workers,[22] may allow for better hydration and higher photocurrent efficiencies. Work along these lines is currently in progress.

Acknowledgment. We thank Dr. Gilles Villemeure and Profs. Allen J. Bard and Morton Z. Hoffman for helpful discussions and suggestions. This work was supported by the Division of Chemical Sciences, Office of Basic Energy Sciences, Department of Energy, under contract DE-FG-05-87ER13789. T.E.M. thanks the Alfred P. Sloan Foundation for support in the form of a Research Fellowship.

(19) Quenching efficiencies could not be estimated to greater accuracy because the effect of multiply charged anions, such as $Mo(CN)_8^{4-}$ and $Fe(CN)_6^{4-}$, on the nonradiative decay rate of pillared-clay-supported $Ru(bpy)_3^{2+}$ could not be evaluated from steady-state measurements.

(20) Mallouk, T. E.; Krueger, J. S.; Mayer, J. E.; Dymond, C. M. G. *Inorg. Chem.*, in press.

(21) Ueno, F. B.; Sasaki, Y.; Ito, T.; Saito, K. *J. Chem. Soc., Chem. Commun.* **1982**, 328.

(22) (a) Montgomery, D. D.; Tsuchida, E.; Shigehara, K.; Anson, F. C. *J. Am. Chem. Soc.* **1984**, *106*, 7991. (b) Montgomery, D. D.; Anson, F. C. *J. Am. Chem. Soc.* **1985**, *107*, 3431.